Plant, Cell and Environment (2009) **32**, 237–249 doi: 10.1111/j.1365-3040.2008.01916.x

Quantifying the three main components of salinity tolerance in cereals

KARTHIKA RAJENDRAN, MARK TESTER & STUART J. ROY

The Australian Centre for Plant Functional Genomics and the University of Adelaide, PMB1, Glen Osmond, SA 5064, Australia

ABSTRACT

Salinity stress is a major factor inhibiting cereal yield throughout the world. Tolerance to salinity stress can be considered to contain three main components: Na^+ exclusion, tolerance to Na^+ in the tissues and osmotic tolerance. To date, most experimental work on salinity tolerance in cereals has focused on Na^+ exclusion due in part to its ease of measurement. It has become apparent, however, that Na^+ exclusion is not the sole mechanism for salinity tolerance in cereals, and research needs to expand to study osmotic tolerance and tissue tolerance. Here, we develop assays for high throughput quantification of Na^+ exclusion, Na^+ tissue tolerance and osmotic tolerance in 12 *Triticum monococcum* accessions, mainly using commercially available image capture and analysis equipment. We show that different lines use different combinations of the three tolerance mechanisms to increase their total salinity tolerance, with a positive correlation observed between a plant's total salinity tolerance and the sum of its proficiency in Na^+ exclusion, osmotic tolerance and tissue tolerance. The assays developed in this study can be easily adapted for other cereals and used in high throughput, forward genetic experiments to elucidate the molecular basis of these components of salinity tolerance.

Key-words: *Triticum monococcum*; LemnaTec Scanalyzer; Na^+ exclusion; Na^+ tissue tolerance; osmotic tolerance.

INTRODUCTION

Salinity is a significant problem affecting agriculture worldwide and is predicted to become a larger problem in the coming decades (http://www.fao.org/ag/agl/agll/spush/). To combat this problem, the salinity tolerance of crop plants needs to be increased to enable them to grow on marginal areas already affected by salinity. Use of both genetic manipulation and traditional breeding approaches will be required to develop salt-tolerant cultivars better able to cope with the increasing soil salinity constraints. One such approach is to introduce traits and genes from near relatives of current crop cultivars that have not undergone strong human-imposed selective pressures, but have instead adapted to the highly variable environments in the Middle East (Dubcovsky *et al.* 1996a).

The A^m genome of *Triticum monococcum* represents a large resource of untapped genetic variability for numerous plant traits which could be introduced into modern-day bread and durum wheat cultivars. The use of *T. monococcum* or its closely related wild relative *Triticum boeoticum* has already been used to find traits which can be used to improve cultivated wheat varieties, for example, bread-making quality (Rogers *et al.* 1997), kernel softness (See, Giroux & Gill 2004), leaf rust (Anker, Buntjer & Niks 2001; Sodkiewicz, Strzembicka & Apolinarska 2008), seed dormancy (Sodkiewicz 2002) Zn efficiency uptake (Cakmak *et al.* 1999) and frost tolerance (Knox *et al.* 2008). There exists, therefore, the possibility of the discovery of novel genes in *T. monococcum* which may improve the salinity tolerance of current wheat cultivars. Indeed the loci, *Nax1* and *Nax2*, which are reported to increase the salinity tolerance of durum wheat, have come from *T. monococcum* (James, Davenport & Munns 2006; Byrt *et al.* 2007).

Salinity stress affects crop growth, yield and productivity (Tester & Davenport 2003; Munns & Tester 2008). Sodium (Na^+) and chloride (Cl^-) are the two key ions responsible for both osmotic and ion-specific damage that significantly reduces crop growth and yield (Munns & Tester 2008). The osmotic effects of salinity stress can be observed immediately after salt application and are believed to continue for the duration of exposure, resulting in inhibited cell expansion and cell division, as well as stomatal closure (Flowers, Hajibagherp & Yeo 1991; Yeo *et al.* 1991; Passioura & Munns 2000; Fricke & Peters 2002; Munns 2002; Munns & Tester 2008). Ionic stress results in premature senescence of older leaves and in toxicity symptoms (chlorosis, necrosis) in mature leaves (Munns 2002; Tester & Davenport 2003; Munns, James & Lauchli 2006), due to high Na^+ concentrations disrupting protein synthesis and interfering with enzyme activity (Bhandal, Malik & Bourne 1988; Blaha *et al.* 2000).

Plants have evolved three main mechanisms to enable them to tolerate salinity stress. Osmotic tolerance involves the plant's ability to tolerate the drought aspect of salinity stress and to maintain leaf expansion and stomatal conductance. While the mechanisms involved in this process are not fully understood, it can be demonstrated that the plant's response to the osmotic stress is independent of nutrient

Correspondence: M. Tester. Fax: +61 883037102; e-mail: mark.tester@acpfg.com.au

levels in the growth medium (Hu *et al.* 2007). The second two mechanisms of tolerance involve the ability to reduce the ionic stress on the plant by minimizing the amount of Na^+ that accumulates in the cytosol of cells, particularly those in the transpiring leaves. The first mechanism works by excluding Na^+ from leaves (Tester & Davenport 2003; Møller & Tester 2007; Munns & Tester 2008), the second by efficiently compartmentalizing Na^+ in the vacuole or in particular cell types where the damage to metabolism is kept to a minimum (Apse *et al.* 1999; Pardo *et al.* 2006; Munns & Tester 2008). Both processes involve up- and down-regulation of the expression of specific ion channels and transporters, allowing the control of Na^+ transport throughout the plant (Apse *et al.* 1999; Qiu *et al.* 2002; Shi *et al.* 2002, 2003; Sunarpi *et al.* 2005; Rus *et al.* 2006; Davenport *et al.* 2007).

It has been suggested that salinity tolerance in wheat (Gorham 1990; Schachtman & Munns 1992; Munns & James 2003; Poustini & Siosemardeh 2004) and other cereals (Forster 2001; Zhu, Kinet & Lutts 2001; Wei *et al.* 2003; Garthwaite, von Bothmer & Colmer 2005) is particularly associated with the ability to exclude Na^+ from the shoot. To date, research into improving the salinity tolerance of wheat cultivars has already identified mechanisms for Na^+ exclusion such as the *Kna1* locus on chromosome 4D of bread wheat (Dubcovsky *et al.* 1996b) and the *Nax1* and *Nax2* loci in durum wheat (James *et al.* 2006; Byrt *et al.* 2007). It is, however, becoming increasingly apparent that osmotic tolerance and Na^+ tissue tolerance may also play an important role in the salinity tolerance of cereals, with evidence mounting that there is not necessarily an inverse relationship between shoot Na^+ concentrations and plant salinity tolerance, such as for certain Australian cultivars of wheat (Genc, McDonald & Tester 2007).

A key factor in why little work has taken place investigating tissue tolerance and osmotic tolerance in cereals is the ease of obtaining accurate and repeatable measurements. In order to most accurately distinguish the effects of osmotic tolerance (which have a rapid onset) from Na^+-specific tolerance (which builds up over many days), it is necessary to make daily observations of plant growth over time. To then, distinguish between measures for Na^+ exclusion and Na^+ tissue tolerance, one needs to consider both shoot Na^+ concentrations and measures of Na^+-induced leaf death after prolonged exposure to high Na^+ (Munns & Tester 2008). Plants which have high osmotic tolerance will maintain growth rates, particularly over the first few days after exposure to Na^+, whereas those with low leaf senescence and either low or high shoot Na^+ concentrations will be Na^+ excluders or tissue tolerators, respectively. While it is relatively easy to obtain measures of Na^+ exclusion by measuring shoot or leaf blade Na^+ accumulation under salt stress conditions, such as by flame photometry or inductively coupled plasma spectrometry (Ren *et al.* 2005; Rus *et al.* 2006; Davenport *et al.* 2007), measurements of both tissue and osmotic tolerance are harder to obtain using destructive measurements. While it is possible to make estimates of osmotic stress using measures of stomatal conductance (James *et al.* 2002, 2008), and it has been demonstrated that a good correlation exists between conductance and growth rate, as measured destructively between two time-points (James *et al.* 2008), stomatal conductance nevertheless remains an indirect measure of growth rate.

In the experiments described in the current work, commercially available image capture and analysis equipment (LemnaTec 'Scanalyzer 3D': see http://www.lemnatec.de/scanalyzer_gh.htm) is used to take non-destructive measurements of both plant growth and health. Two side view and one top view digital photographs were taken of the plant to calculate plant area and colour, parameters which can be used to measure growth and leaf health. This system has been used extensively in unpublished studies by private companies, but we know of no published refereed report using this approach. In the work presented here, this image capture and analysis equipment is used, in combination with flame photometery, to develop quantitative assays for measuring osmotic tolerance, Na^+ exclusion and Na^+ tissue tolerance in different accessions of *T. monococcum*. Using these assays, it is apparent that there is no preferential tolerance mechanism in *T. monococcum*, with some lines having good Na^+ exclusion while others are Na^+ tissue tolerators. Several of the lines also show good osmotic tolerance. With such assays in place, novel genes for the dissected components of salinity tolerance can now be identified through forward genetic approaches.

MATERIALS AND METHODS

Plant material and growth conditions

In order to seek variation in salinity tolerance mechanisms, 12 cultivated einkorn wheat (*T. monococcum* ssp. *monococcum*) accessions were screened. The seed was provided by the Australian Winter Cereal Collection (Tamworth, Australia) and Rothamsted Research (Harpenden, UK). A list of the accessions used in these experiments is presented in Supporting Information Table S1.

Seeds were germinated at room temperature for a maximum of 4 d on moist filter paper in Petri dishes wrapped in polythene bags to maintain high humidity. When the plumule was approximately 2 cm long, seedlings were transplanted into a supported hydroponics setup (Genc *et al.* 2007). If individual plants germinated quickly, they were stored at 4 °C until all plants reached the same size. Individual plants were then placed into separate PVC tubes (280 mm long × 45 mm diameter) that were filled with cylindrical black polycarbonate pellets, and placed into a 25 L bath above a reservoir tank (Supporting Information Fig. S1a). Modified Hoagland's solution (Genc *et al.* 2007) was pumped from the reservoir to the 25 L bath in a 20 min fill, 20 min drain cycle. The nutrient solution was changed every 7 d. Plants were grown in two separate experiments in a glasshouse, in the South Australian winter and spring, with max/min temperatures of 28 °C during the day and 15 °C during the night. A selection of lines were grown in both experiments to monitor for effects on plant growth arising

from the need to do the current experiment in two stages. The work described in this paper is a preliminary experiment, preparatory for undertaking large-scale automated screening in a new facility called 'The Plant Accelerator', which is currently being built (see http://www.plantphenomics.org.au/).

Salinity stress and destructive measurements of plant growth

Ten replicates of each accession were randomly distributed in both salt and control trolleys. At the time of fourth leaf emergence, approximately 12 d after germination, NaCl was added to the hydroponics in 25 mM increments over 1.5 d to a final concentration of 75 mM. To keep the levels of free Ca^{2+} constant with control conditions (Tester & Davenport 2003), an additional 1.71 mM $CaCl_2$ was added. After 19 d of Na^+ stress, the fourth leaf blade and remaining shoot were harvested. The total shoot fresh weight (FW) was measured before the tissue was dried at 75 °C for 3 d to obtain the dry weight. Total leaf blade area was calculated by harvesting all the leaf blades from the plant, laying them out flat and measuring their area using a planimeter (PATON electronic belt driven planimeter, CSIRO, Canberra, Australia).

Non-destructive plant growth analysis

Non-destructive measurements of plant growth were taken periodically through the experimental time course using a plant image capture and analysis system (Scanalyzer 3D, LemnaTec, Würselen, Germany; http://www.lemnatec.de/scanalyzer_gh.htm; see Supporting Information Fig. S1b). Three high-resolution images were taken of every plant, one photograph from the top and two from the side at a 90° horizontal rotation (Supporting Information Fig. S1c–e). These pictures were used to produce false colour images where the plant could be identified from the background of the photograph for calculation of total plant area. The projected shoot 'area' was calculated by an image-based leaf sum (IBLS) model, where the three areas measured by the imaging system were summed and used as a parameter for non-destructive plant growth analysis. Plant health was determined by categorizing leaf colour into healthy (green), senescent (yellow) and necrotic (brown). For each category, several representative areas of leaf health were defined on an image of an individual *T. monococcum* plant taken after 19 d of salt stress. These parameters were then used to determine the health of all samples (Supporting Information Fig. S1f–h).

Measurements of Na^+ exclusion, Na^+ tissue tolerance and osmotic tolerance

A plant's ability to exclude Na^+ was determined by measuring the concentration of Na^+ in the fourth fully expanded leaf blade at the time of harvest. The fourth leaf blade was selected as it was the first leaf to fully develop under salt-stressed conditions in our experiment. Na^+ accumulation was measured in a single leaf, rather than the whole shoot, to ensure measurements were focused on the effects of Na^+ on the primary photosynthetic tissues and not on tissues such as the sheath which can be used for Na^+ storage (James *et al.* 2006). Samples were harvested, fresh and dry weights were recorded and then digested in 10 mL of 1% HNO_3 at 95 °C for 4 h in a 54-well HotBlock (Environmental Express, Mount Pleasant, SC, USA). The concentration of Na^+ in the digested samples was determined using a flame photometer (model 420, Sherwood, Cambridge, UK). Plants which accumulated low levels of Na^+ in their shoots were deemed excluders.

To screen for osmotic tolerance, the reduction in plant growth after the addition of NaCl relative to the control was determined non-destructively using the imaging system. Once a day, for the first 5–7 d after the initial 25 mM incremental NaCl application, plant area was measured and growth rate was calculated. Plants growing in the winter were measured for the first 7 d, while those grown in the spring were measured for 5 d. Plants which maintained similar growth rates under stress conditions when compared to control plants were deemed osmotic tolerant. After these initial observations, measurements of plant area were taken three times a week until the plants were approximately 4 weeks old.

To assess Na^+ tissue tolerance, false colour images taken on the 19th day after salt application were used to determine the area of healthy leaf and the area of senescing leaf. These measurements were combined with the leaf Na^+ concentrations to relate the amount of leaf damage/death with leaf Na^+ concentrations. Plants with low leaf damage and high leaf Na^+ concentrations were determined to have high tissue tolerance, while those with high leaf damage and high or low Na^+ concentrations were deemed sensitive.

Statistical analysis and development of a salt tolerance index

Means, standard error of the mean (SEM) and exponential equations for curve fitting were all performed using Microsoft Excel. To determine total salinity tolerance from the indices, the Na^+ exclusion, osmotic tolerance and tissue tolerance indices generated in this study were combined to generate a total plant salinity tolerance index. Multiple regression analysis was performed using GenStat version 10 (VSN International, Hemel, UK) on the individual tolerance indices to determine the weighting to apply to each individual mechanism, using the reduction in shoot area as the dependent variable.

RESULTS

Suitability of images for estimating plant growth

The advantage of using imaging technologies is that information on plants can be collected non-destructively and

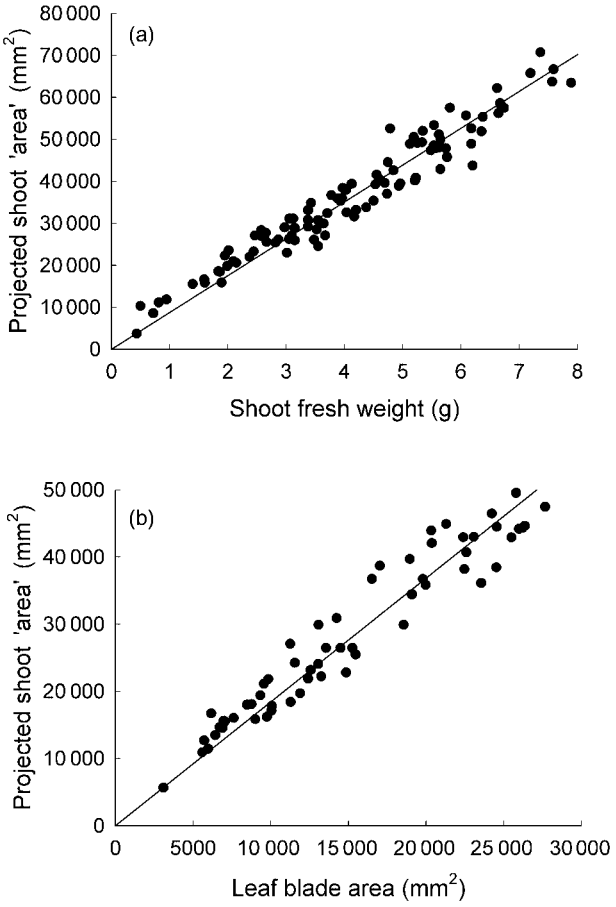

Figure 1. Comparison of projected areas measured by the imaging system with conventional measures of shoot size. (a) Comparison of Scanalyzer projected shoot 'area' (mm^2) against destructively harvested fresh shoot biomass (g) of plants of *Triticum monococcum*. A positive relationship ($r^2 = 0.94$) was observed between destructive and non-destructive growth measurements ($n = 101$). (b) Comparison of Scanalyzer projected shoot 'area' (mm^2) against the leaf blade area measured using a planimeter (mm^2). A positive relationship ($r^2 = 0.92$) was observed between the two different methods for calculating leaf area ($n = 59$). All plants were 31-day-old and had been grown in either 0 or 75 mM NaCl for 19 d.

used to calculate growth rates as well as some components of plant function, that is, defined here as plant 'health'. However, it is first necessary to demonstrate that the 'areas' calculated from the captured images are an adequate measure of growth when compared to conventional destructive measures. The 'areas' measured for numerous *T. monococcum* plants at different growth stages were compared with the total shoot FW and the leaf blade area of the same plants, as measured with a physical balance and a planimeter. For both FW (Fig. 1a) and planimeter area (Fig. 1b), there was a strong linear relationship with the 'area' calculated by the imaging system, with r^2 values of 0.94 and 0.92, respectively. The deviation of the slope from 1 in Fig. 1b can be explained by the additional area provided by the plant's sheath that was not measured using the planimeter. Repeated measurements ($n = 10$) of the same plant at both early (17 d) and later (31 d) growth stages demonstrated that the imaging system consistently obtained repeatable measurements (Table 1), with the SEM to be much less than 1% of the mean. The use of two side images and one top image appears to be sufficient to account for overlapping leaves in large plants, and the information from the imaging equipment can be used confidently to measure plant growth rates.

Determination of total plant salinity tolerance

Prior to demonstrating the value of new assays for measuring the individual mechanisms involved in salinity tolerance, it was necessary to establish the total plant tolerance of the *T. monococcum* accessions studied. Conventionally, total plant salinity tolerance is measured destructively at the end of the experimental period, by comparing the weight of control plants against those grown in salt-stressed conditions. As there is a good correlation between plant weight and the 'area' measured by the imaging equipment (Fig. 1a), salinity tolerance can be determined at the end of the experimental period by dividing the average 'area' of an accession under salinity stress by that of the average 'area' of the same accession under control conditions. Accessions AUS 18755-4 and MDR 308 and, to a lesser extent, AUS 90436 and MDR 043, have relatively high salinity tolerance and a good ability to maintain high growth rates under salinity stress when compared to control plants (Table 2). In contrast, accessions AUS 18758 and AUS 90423 are salt-sensitive plants, showing a 67% reduction in growth rate compared to the controls when grown in 75 mM NaCl. Although these results clearly demonstrate which accessions are better able to maintain growth rates under saline conditions, the results do not indicate which salinity tolerance mechanism(s) are responsible for the observed tolerance.

Development of a Na^+ exclusion index

The final concentration of Na^+ in the fully expanded fourth leaf blade of a 31-day-old plant, after 19 d of exposure to 75 mM NaCl, was used to develop a Na^+ exclusion index. There was a large variation in all *T. monococcum* accessions studied, ranging from the low Na^+ accumulators, MDR 308 and AUS 90436 (which accumulate 39 ± 2 and 64 ± 31 mM tissue Na^+ concentrations, respectively) to the high accumulating accessions, AUS 18755-4 and MDR 043, which accumulate 224 ± 44 and 259 ± 32 mM, respectively (Table 3). While there was variation in the water content of each leaf between the accessions, this does not appear to be correlated with Na^+ concentration (Table 3). To develop a standardized Na^+ exclusion index, with the best excluder having a value of 1 and the worst a theoretical value of 0, the fourth leaf Na^+ concentration of the lowest accumulating accession was divided by the Na^+ concentration of the line in question (Table 3). Using this scale, it can be seen that MDR 308 was the best *T. monococcum* Na^+ excluder in this study, while MDR 043 was the worst.

Table 1. Calculations of Scanalyzer machine error

	17 d		31 d	
Plant number	Projected shoot 'area' (mm^2)	SE as % of mean	Projected shoot 'area' (mm^2)	SE as % of mean
1	3179	0.30	21 118	0.60
2	4036	0.20	30 100	0.30
3	4096	0.20	37 196	0.20
4	5329	0.40	38 929	0.06
5	5383	0.10	46 908	0.20

The same individual plant shoot 'area' was measured repeatedly ($n = 10$) for five different plants at both 17 and 31 d to obtain an estimate of the error in the measurement of 'area'. Results are presented as the mean 'area' and SE as a percentage of the mean.

Table 2. Total plant salinity tolerance

	Projected shoot 'area' ($\times 10^3$ mm^2)		
Accession	0 mM NaCl	75 mM NaCl	Salinity tolerance
AUS 18758[a]	37.5 ± 2.5	12.4 ± 3.1	0.33
AUS 90423[b]	41.7 ± 1.1	13.4 ± 3.2	0.33
MDR 002[b]	28.0 ± 5.0	13.4 ± 1.2	0.48
MDR 044-1[b]	44.2 ± 1.1	22.0 ± 0.9	0.50
AUS 18763[a]	35.9 ± 2.9	18.4 ± 2.8	0.51
MDR 044-2[a]	48.6 ± 2.0	25.1 ± 1.6	0.52
AUS 16273[b]	43.6 ± 1.7	22.4 ± 2.2	0.52
MDR 037[a]	50.0 ± 5.1	27.8 ± 4.9	0.55
MDR 043[a]	47.8 ± 4.5	29.8 ± 2.2	0.62
AUS 90436[b]	36.7 ± 4.2	23.9 ± 1.5	0.65
MDR 308[b]	38.9 ± 2.6	26.4 ± 8.6	0.68
AUS 18755-4[a]	43.8 ± 7.6	31.3 ± 1.4	0.71

[a]Plants grown in spring.
[b]Plants grown in winter.
Plant salinity tolerance calculated using the ratio of projected shoot 'area' of 31-day-old *Triticum monococcum* lines grown for 19 d in 75 mM NaCl, relative to 0 mM NaCl-grown plants. Values are mean ± SE of 6–10 replicates.

Table 3. Calculation of Na^+ exclusion index

Accession	Mass of tissue water (g) per g FW of tissue	Fourth leaf $[Na^+]$ on tissue water basis (mM)	Na^+ exclusion index
AUS 18758[a]	0.85 ± 0.02	188 ± 29	0.20
AUS 90423[b]	0.76 ± 0.03	206 ± 81	0.19
MDR 002[b]	0.79 ± 0.03	114 ± 4	0.34
MDR 044-1[b]	0.79 ± 0.01	136 ± 4	0.29
AUS 18763[a]	0.78 ± 0.04	177 ± 60	0.22
MDR 044-2[a]	0.79 ± 0.01	204 ± 26	0.19
AUS 16273[b]	0.77 ± 0.04	115 ± 55	0.34
MDR 037[a]	0.86 ± 0.02	185 ± 55	0.21
MDR 043[a]	0.87 ± 0.05	259 ± 32	0.15
AUS 90436[b]	0.80 ± 0.01	64 ± 31	0.60
MDR 308[b]	0.78 ± 0.03	39 ± 2	1.00
AUS 18755-4[a]	0.86 ± 0.01	224 ± 44	0.17

[a]Plants grown in spring.
[b]Plants grown in winter.
Fourth leaf Na^+ concentrations (mM) in 31-day-old hydroponically grown *Triticum monococcum* accessions, grown for 19 d in 75 mM NaCl, were used to calculate the Na^+ exclusion index. The index was calculated by dividing the Na^+ concentration in the lowest Na^+ accumulating line by that of the line in question. Mass of tissue water per unit mass of tissue and fourth leaf Na^+ concentrations are expressed as the mean ± SEM ($n = 5$–9).

Development of an osmotic tolerance screen

Under control conditions, *T. monococcum* plants were measured regularly and non-destructively, and showed approximately exponential growth over the experimental period, as illustrated by AUS 16273 (Fig. 2a). Under 75 mM NaCl stress, however, there is, for most lines, a large reduction in plant growth for the first 7 d after salt application, before the growth rate recovers, if it recovers at all (Fig. 2a; Supporting Information Table S2). This initial reduction in plant growth rate can be mainly attributed to osmotic stress and is independent of the accumulation of Na^+ in the shoot tissues (Munns & Tester 2008). The extent of this growth reduction over the first 5–7 d varies between accessions, with some showing only minor reductions in growth rate after salt application, while in others the rate is almost halved (Fig. 2b & Fig. 2c, respectively; Supporting Information Table S2). To develop an osmotic tolerance index, the growth rate for the first 5–7 d after salt application in salt-treated plants was divided by the growth rate of the control plants for the same period. The results were then standardized by dividing the line's osmotic tolerance value by that of the best osmotic tolerator to generate an index where the most osmotic tolerant accession had an index value of 1, with the theoretically most sensitive having an index value of 0. Two different growth periods were used between two experiments because of the different seasons the plants were grown. Each of the two experiments consisted of six accessions, with line MDR 044 grown in both (MDR 044-1 and MDR 044-2, respectively) to allow comparison between experiments. Using the osmotic index, it was clear that accessions AUS 90436, MDR 043 and AUS 18755-4 had the greatest osmotic tolerance, showing minimal growth rate reduction after salt application, while AUS 16273 and MDR 044-1 were the most sensitive and showed a greater than 50% reduction in growth rates (Table 4).

It would be much better for future forward genetic studies, though, if osmotic tolerance could be determined without the need to grow unstressed controls. This would help the phenotyping of populations of plants, such as F_2 mapping populations, where every individual is unique. In this case, to generate an osmotic tolerance index, growth rate of the plants after salt application was divided by the plant's growth rate before salt addition (Fig. 3a). Unfortunately, data were collected from only six lines before salt application to enable pre-salt growth rates to be generated. Nevertheless, when the two osmotic indices are compared, a good correlation between them can be seen, with an r^2 of 0.83 (Fig. 3b; Supporting Information Table S3).

Development of a tissue tolerance index

Plants which are tissue tolerant have the ability to compartmentalize Na^+ in the shoot into particular cell types and organelles, preventing it from building up in the cytosol, while those plants that are less effective at compartmentalization will display higher rates of leaf senescence and necrosis for a given tissue concentration of Na^+. A measure

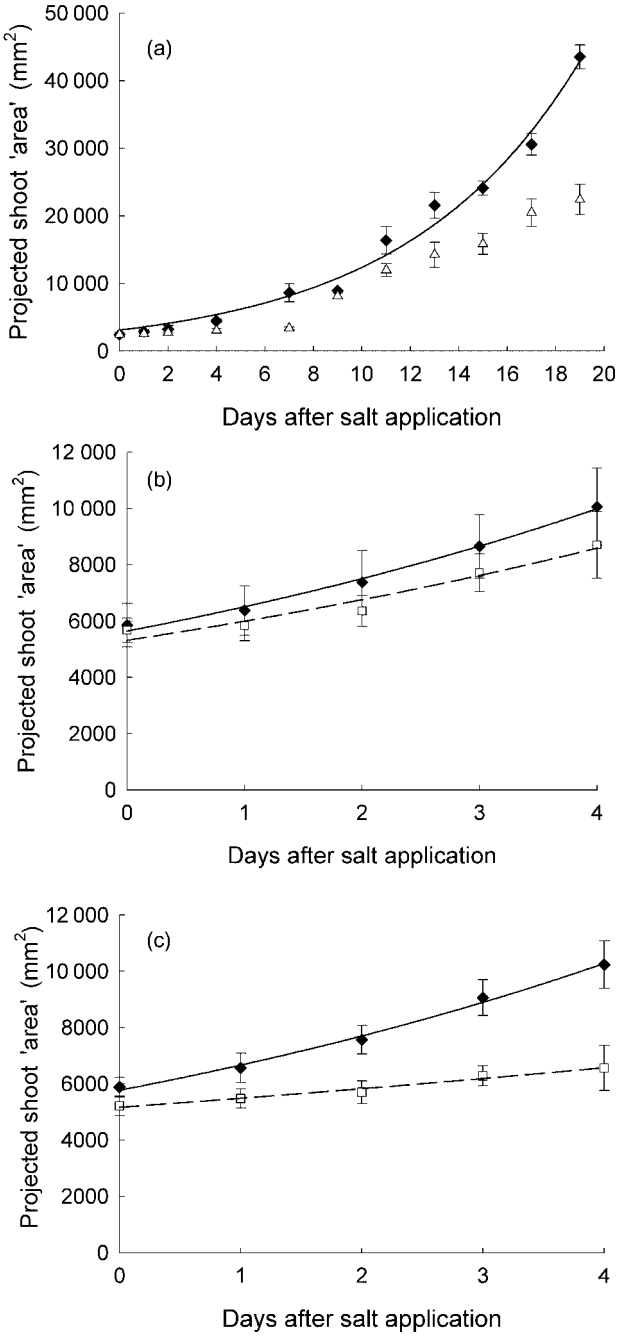

Figure 2. (a) Growth response of 12 d *Triticum monococcum* accession AUS 16273 after addition of either 0 (◆) or 75 mM (△) NaCl at $t = 0$. Each observation is the mean ± SE ($n = 7$–9). For calculating the reductions in growth rate because of osmotic stress, growth was measured for the first 4 d after addition of either 0 or 75 mM NaCl, and rate of growth in each condition calculated. Examples are shown for (b) (MDR 043) with mean relative growth rates of 0.14 and 0.11 in 0 (◆) and 75 mM (□) NaCl, respectively, and for (c) (MDR 044-2) with mean relative growth rates of 0.14 and 0.06 in 0 (◆) or 75 mM (□) NaCl, respectively. Results are the mean ± SEM ($n = 9$).

Table 4. Calculation of osmotic tolerance index

Accession	Mean relative growth rate		Osmotic tolerance (Y/X)	Osmotic tolerance index
	Control (X) (d^{-1})	75 mM NaCl (Y) (d^{-1})		
AUS 18758[a]	0.15	0.09	0.60	0.72
AUS 90423[b]	0.08	0.04	0.50	0.60
MDR 002[b]	0.08	0.04	0.50	0.60
MDR 044-1[b]	0.14	0.05	0.36	0.43
AUS 18763[a]	0.13	0.09	0.69	0.83
MDR 044-2[a]	0.14	0.06	0.43	0.52
AUS 16273[b]	0.11	0.04	0.36	0.43
MDR 037[a]	0.13	0.06	0.46	0.55
MDR 043[a]	0.14	0.11	0.79	0.95
AUS 90436[b]	0.06	0.05	0.83	1.00
MDR 308[b]	0.10	0.06	0.60	0.72
AUS 18755-4[a]	0.14	0.11	0.79	0.95

[a]Plants grown in spring.
[b]Plants grown in winter.
Measurements of relative plant growth rate (calculated from projected shoot area) from 0 to 5, or 0 to 7 d after the first 25 mM salt application were used to determine osmotic tolerance. Osmotic tolerance was calculated by dividing mean relative growth rate of plants grown in 75 mM NaCl (Y) by the growth rate of plants in 0 mM NaCl (X). The osmotic tolerance index was calculated by dividing the line with the highest osmotic tolerance with that of the line to be tested.

for tissue tolerance, therefore, needs to consider the amount of Na^+ accumulating in the leaf as well as the leaf's health. Using the imaging system, it is possible to create false colour images of plants from the real images using previously established parameters for healthy (green), senescing (yellow) and necrotic (brown) tissue, and calculate the relative area of each in both control and salt-stressed plants (see Fig. 4a–c, for an example). Use of the flame photometer on harvested fourth leaf samples after 19 d growth in 75 mM NaCl allowed the determination of leaf 4 Na^+ concentrations.

Before a tissue tolerance index could be calculated, it was necessary to account for natural leaf senescence and necrosis (together called 'senescence' from now), in salt-stressed plants in order to determine the extent of Na^+-induced senescence. A correlation was established between plant size and senescence in control plants by calculating shoot area as well as total area of senescence after 31 d of growth (Fig. 4d). A positive correlation between total shoot area and senescent shoot area was found ($y = 0.32032x - 2140$), which was then used to estimate the amount of natural senescence occurring in salt-stressed plants, thereby enabling us to calculate the likely salt-induced senescent area. Plants with a low degree of salt-induced senescence and high salt concentrations were deemed to be tissue tolerant (Table 5). Assuming the effect of Na^+ concentration in leaf 4 occurs linearly, the tissue tolerance index can therefore be calculated by:

$$\text{Tissue tolerance} = \left(\frac{\text{Total shoot area} - \text{Predicted salt induced senescence}}{\text{Total shoot area}} \right) \times \frac{1}{4^{\text{th}}\ \text{leaf}\ [Na^+]}$$

Again, the index was scaled to range between 0 and 1 by dividing the tolerance value of the line in question by the tolerance value of the best tolerator. Thus, the best tissue-tolerating plant would have a value of 1, while the theoretical worst tolerator would have a value of 0. For the *T. monococcum* lines in this study, MDR 043 and AUS 18755-4 were the most tissue-tolerant accessions, while MDR 002 and MDR 308 were the least tissue tolerant.

Total tolerance index versus conventional tolerance measurements

To determine total salinity tolerance from the indices, the Na^+ exclusion, osmotic tolerance and tissue tolerance indices were combined to generate a total plant salinity tolerance index using multiple regression analysis to determine the weighting to apply to each individual mechanism. From these results, the following formula for total plant tolerance was derived that was applicable to the plants used in the current experiment, with a significance level of $P = 0.043$: total plant salinity tolerance = (0.5 × exclusion index) + (0.14 × osmotic tolerance index) + (0.38 × tissue tolerance index) + 0.06. This equation was then applied to the results obtained for each accession used in this study to generate its total salinity tolerance (Table 6). From this analysis, MDR 308 and MDR 043 were the best total salt tolerators as they make better use of key tolerance mechanisms. By plotting the salinity tolerance of lines, as measured by the reduction in growth (Table 2), against the predicted total salinity tolerance estimated from the contribution of the three tolerance mechanisms (Table 6), a strong relationship was found between predicted estimates of plant tolerance and the tolerance measured directly (Fig. 5).

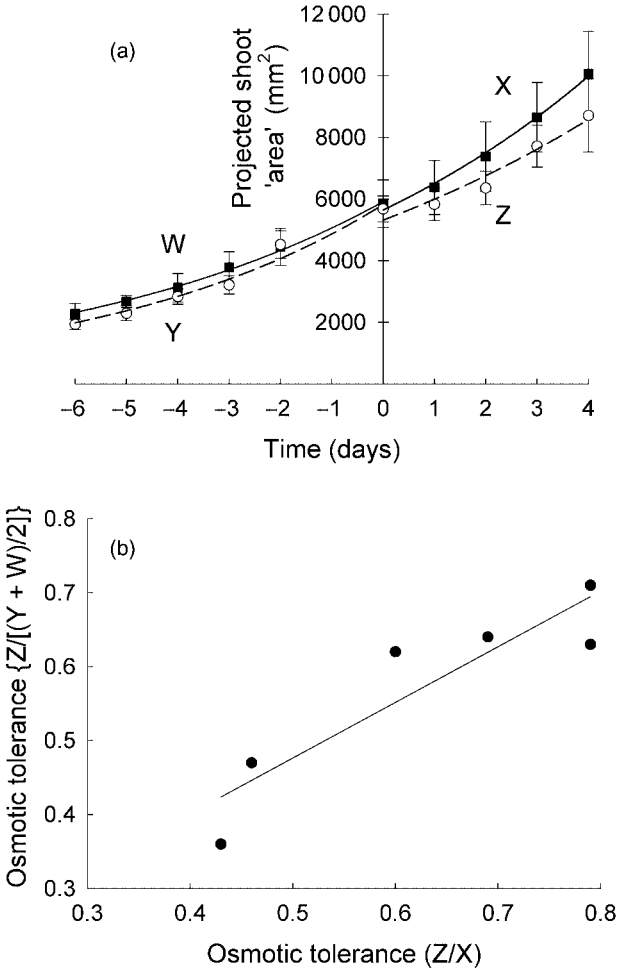

Figure 3. Creation of an index for measuring osmotic tolerance using growth of the same individual plant before and after salt application. (a) Growth of accession MDR 043 in both 0 mM (■) and 75 mM (○) NaCl before and after salt application. Results are mean ± SEM ($n = 9$). Osmotic tolerance can be determined by either dividing the mean relative growth rate of 75 mM plants (part Z on graph) by mean relative growth rates of 0 mM plants (part X), or by dividing relative growth rates of 75 mM plants (part Z) by growth before salt application (average of parts W and Y). (b) Relationship between calculating osmotic tolerance index for six accessions by dividing relative growth rates of Z by X, or relative growth rate Z by the average growth rate before addition of salt (W and Y). A good association ($r^2 = 0.83$) between the two methods was found.

DISCUSSION

Using imaging technologies for screening plants

Plant salinity tolerance is usually measured at the end of the experimental period by comparing the weight or yield of control plants against those grown in salt-stressed conditions (Munns & Rawson 1999; Genc *et al.* 2007). Unfortunately, this method is not only destructive, which prevents making multiple observations of the same plant over an experimental period and stops a plant of interest being taken through to seed, but destructive measurements also do not allow a dissection of the three mechanisms of salinity tolerance: Na^+ exclusion, Na^+ tissue tolerance and/or osmotic tolerance. Consequently, the ability to take non-destructive digital images of a plant and reliably extrapolate its surface area for measures of plant growth and health, is a significant step forward. The work presented here clearly demonstrates that the LemnaTec Scanalyzer 3D can reliably make accurate estimates of a plant's growth (Fig. 1; Table 1), and allows us to easily separate the three main mechanisms involved in salinity tolerance and identify the primary mechanism(s) that an individual plant uses (Figs 2 & 3; Tables 3–6). Although the data presented here are solely for *T. monococcum*, we are also successfully using the Scanalyzer to make similar observations in both wheat and barley, which have simpler morphology (data not shown). For both large and small *T. monococcum* plants, there was a clear correlation between the projected 'area' measured by the image analysis system and both the measurements of plant size and weight (Fig. 1). In addition, repeated analysis of the same plant demonstrates the reliability and low level of error of this technique and how factors that might have resulted in an underestimation of plant area, such as shading of leaves from the camera, were adequately addressed by having two side- and one top view image (Table 1), at least for plants of the size and geometry used in the present study.

Importantly, it was necessary to develop a system for measuring osmotic tolerance that did not depend on plants grown in control conditions, essential when working with populations of plants such as F_2 mapping populations, where each individual is different. For screening populations for Na^+ accumulation and Na^+-induced leaf damage, it is accepted that it is not necessary to compare data between Na^+-stressed and control plants. However, for measuring differences in growth rates, controls are always necessary (Munns & James 2003). By using the image-capturing device to obtain growth rates of the plant before and after salt stress, we demonstrate that, at least for the stage of growth of the plants in this study, it is possible to accurately measure the reduction in growth rate caused by osmotic stress without the use of control grown plants (Fig. 3b). While we feel that control plants should ideally be grown whenever possible, the assay described here provides a robust alternative if that is not feasible (such as when using segregating populations).

The clear identification of the osmotic phase and ionic phase of plant growth

As demonstrated in Fig. 2a and Supporting Information Table S2, two phases in the growth response of a plant under saline conditions could be distinguished. While control plants show one phase of exponential growth over the experimental period, the growth of plants under saline conditions can be resolved into two phases: an initial response to the salt stress observed over the first 7 d after salt application, and a long-term response that can be

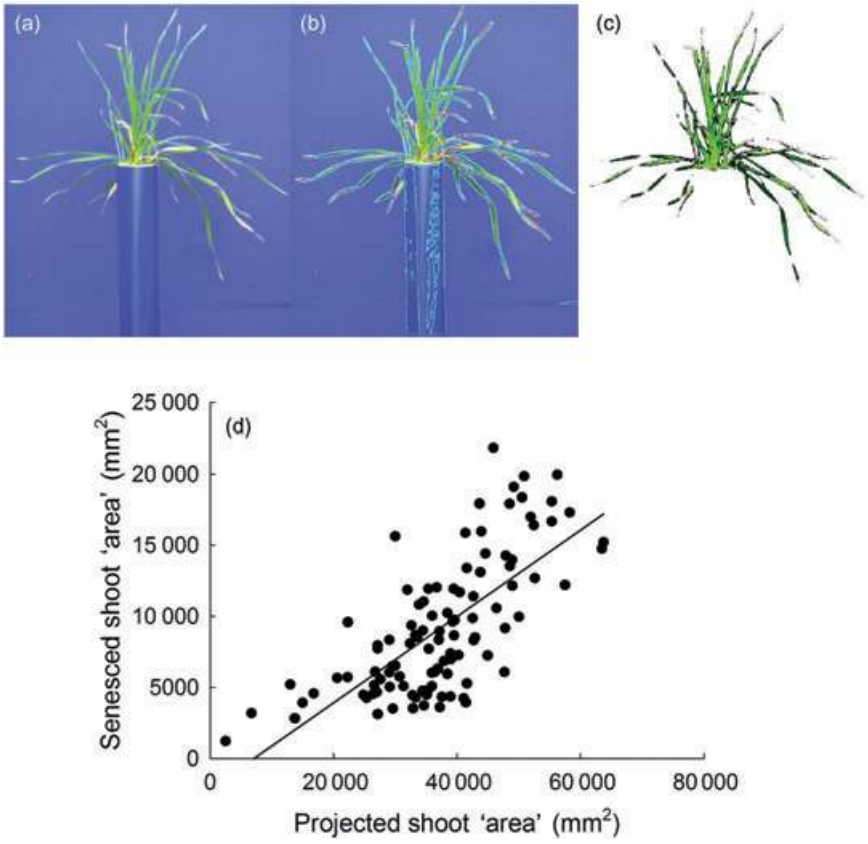

Figure 4. Calculation of rates of natural senescence in plant population. (a) Original digital image of side view of plant taken by the imaging system. (b) Computer-processed image determining location of plant. (c) False colour image used to determine healthy, senescent and necrotic regions on the plant. (d) Plot of shoot area in control grown plants against shoot senescent area ($n = 109$). The slope of the line $y = 0.3032x - 2140.7$ was used to calculate the predicted natural senescence expected in salt-grown plants.

Table 5. Calculation of tissue tolerance index

Accession	Measured 'area' ($\times 10^3$ mm^2)		Predicted senesced area ($\times 10^3$ mm^2)		Fourth leaf [Na^+] (mM)	Tissue tolerance	Tissue tolerance index
	Total shoot	Senesced area	Natural	Salt induced			
AUS 18758[a]	12.4	5.7	1.6	4.1	188	126	0.59
AUS 90423[b]	13.4	8.6	1.9	6.6	206	104	0.49
MDR 002[b]	13.4	8.2	1.9	6.3	114	60	0.28
MDR 044-1[b]	21.9	7.5	4.5	3.0	136	117	0.55
AUS 18763[a]	18.4	8.5	3.4	5.0	177	128	0.60
MDR 044-2[a]	25.1	8.5	5.5	3.1	204	179	0.84
AUS 16273[b]	22.4	8.5	4.7	3.8	115	95	0.44
MDR 037[a]	27.8	13.2	6.3	6.9	184	139	0.65
MDR 043[a]	29.8	12.1	6.9	5.2	259	214	1.00
AUS 90436[b]	23.9	5.5	5.1	0.4	64	63	0.30
MDR 308[b]	26.4	7.5	5.9	1.7	39	36	0.17
AUS 18755-4[a]	31.3	13.2	7.3	5.8	223	182	0.85

[a]Plants grown in spring.
[b]Plants grown in winter.
Tissue tolerance was determined by calculating salt-induced senescence and attributing it to the fourth leaf Na^+ concentration (mM) in 12 lines of *Triticum monococcum* grown for 19 d in 75 mM NaCl. Total and senesced 'areas' of the shoot were determined using the imaging system. The predicted area of natural senescence in salt-treated plants was calculated using the standard curve in Fig. 5 and the equation: predicted natural senescence = (total shoot area $\times$ 0.3032) – 2.14 $\times$ 10^3. Salt-induced senescence = senesced area – predicted natural senescence. Tissue tolerance = [(total shoot area – predicted salt-induced senescence) $\div$ total shoot area] $\times$ fourth leaf [Na^+]. The tissue tolerance index can be calculated by dividing the tissue tolerance of the line in question by that of the highest tolerator (MDR 043).

Table 6. Calculation of predicted total plant salinity tolerance index

Accession	Ratio of shoot growth in 75 mM NaCl relative to control	Na^+ exclusion index	Osmotic tolerance index	Tissue tolerance index	Predicted total salinity tolerance index
AUS 18758[a]	0.33	0.20	0.72	0.59	0.49
AUS 90423[b]	0.33	0.19	0.60	0.49	0.43
MDR 002[b]	0.48	0.34	0.60	0.28	0.42
MDR 044-1[b]	0.50	0.29	0.43	0.55	0.47
AUS 18763[a]	0.51	0.22	0.83	0.60	0.51
MDR 044-2[a]	0.52	0.19	0.52	0.84	0.55
AUS 16273[b]	0.52	0.34	0.43	0.44	0.46
MDR 037[a]	0.55	0.21	0.55	0.65	0.49
MDR 043[a]	0.62	0.15	0.95	1.00	0.65
AUS 90436[b]	0.65	0.60	1.00	0.30	0.61
MDR 308[b]	0.68	1.00	0.72	0.17	0.73
AUS 18755-4[a]	0.71	0.17	0.95	0.85	0.60

[a]Plants grown in spring.
[b]Plants grown in winter.
Multiple regression, using ratio of shoot growth in 75 mM NaCl as the dependent variable, was used to determine an equation for generating predicted total plant tolerance. Predicted total plant tolerance = (0.5 × Na^+ exclusion index) + (0.14 × osmotic tolerance index) + (0.38 × tissue tolerance index) + 0.06.

observed throughout the remainder of the experimental period. The initial growth reduction of plants under salt stress can be mainly attributed to the osmotic effect of the roots being exposed to high NaCl concentrations which result in reductions in cell division and expansion (Munns & Tester 2008).

Interestingly, though, results for the second phase of plant growth under salt stress do not always match those predicted by Munns & Tester (2008). Munns & Tester (2008) hypothesized that once exposed to salt stress, the plants immediately show a reduction in plant growth because of osmotic stress and then maintain that reduction throughout the experimental period, with any additional reduction in growth being attainable to ionic effects (see their Fig. 2). Results show, however, that for many *T. monococcum* lines, although growth rates do reduce over the first 7 d of salt application, they can recover some of their initial pre-salt stressed growth in the longer term (Fig. 2a; Supporting Information Table S2). While this recovery is not complete in all plants, indicating plants are still osmotically stressed, it does indicate that they have some osmotic tolerance mechanisms which allow them to adapt to osmotic stress over a longer period of time, such as by osmotic adjustment, but lack other components of osmotic tolerance, such as the early signalling processes involved in the initial stages of the osmotic response (Munns & Tester 2008). For the purposes of this study, we identified accessions with the ability to maintain growth rates immediately after salt application, such as MDR 043, as having osmotic tolerance as they are able to maintain growth through both the early phases that involve signalling and the later phases that involve slower osmotic adjustment processes. Whatever the longer-term effects of osmotic stress, it is technically easier to quantify osmotic stress early in the experiment, before growth rates are further affected by increases in Na^+ concentration in older leaves (Munns & Tester 2008).

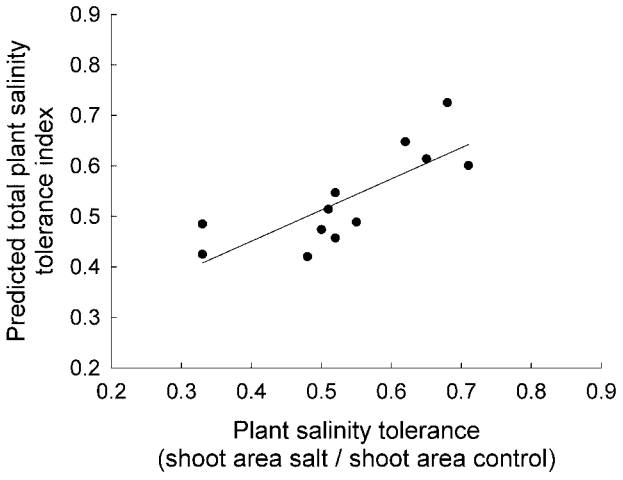

Figure 5. Plot of plant salinity tolerance, as measured by the area under salt stress divided by the area in control conditions (Table 2) against the predicted total plant salinity tolerance using the values generated in Table 6.

Sodium exclusion in *T. monococcum* accessions

As seen in Table 3, accessions such as MDR 308 and AUS 90436 have the ability to manipulate root-to-shoot transport of Na^+ by: (1) reducing the net influx of Na^+ into the root; (2) increasing the net flux of Na^+ from the transpiration stream into the living root cells; (3) compartmentalizing shoot Na^+ into their sheaths and not leaf blades; or (4) a combination of all three mechanisms. Obvious candidate genes for the observed phenotypes would be members of the *HKT* gene

family which are thought to be involved in Na^+ exclusion in *T. monococcum*, after the discovery of two loci, *Nax1* and *Nax2*, in *T. turgidum* spp. *durum* which are believed to have entered the durum AA genome after a cross with *T. monococcum*. It has been shown that *Nax2* is important for reducing root-to-shoot transfer of Na^+ in durum wheat (James *et al.* 2006), and is hypothesized to be *TmHKT1;5-A* (Byrt *et al.* 2007), while *Nax1*, in addition to being important for lowering root-to-shoot Na^+ transfer, is also involved in sequestering Na^+ into the leaf sheath, keeping the levels of Na^+ in the leaf blade low (James *et al.* 2006).

Sodium tissue tolerance in *T. monococcum*

From our results, it appears that the accessions MDR 043 and AUS 18755-4 are both tissue tolerators, accumulating high levels of Na^+ in their shoots while maintaining relatively lower levels of leaf damage compared to other accessions. Both accessions must, therefore, have the ability to reduce the amount of Na^+ accumulating in the cytoplasm of leaf cells, possibly through compartmentation of Na^+ in the vacuole, thereby reducing the toxic effect on cytosolic enzymes and processes (Tester & Davenport 2003). These lines must also be able to accumulate compatible solutes, such as proline and glycine betaine in the cytosol, to balance the osmotic potential in the vacuole (Hasegawa *et al.* 2000; Tester & Davenport 2003). It remains to be seen whether MDR 043 and AUS 18755-4 have higher levels of expression of genes homologous to the *AtNHX* and *AtAVP* families in *Arabidopsis* which are known to increase salinity tolerance in a range of species (Apse *et al.* 1999; Gaxiola *et al.* 2001; Brini *et al.* 2007; Munns & Tester 2008).

Two salinity tolerance mechanisms are better than one: using the tolerance indices

From the data presented, it is clear that while some *T. monococcum* accessions are clearly salt tolerant, they use different tolerance mechanisms to achieve this tolerance. By comparing the total plant tolerance, as measured by shoot area reduction (Table 2), with the Na^+ exclusion index (Table 3) or the tissue tolerance index (Table 5), it can clearly be seen that no particular tolerance mechanism is preferentially used by *T. monococcum*. The best total plant tolerator is AUS 18755-4, which is a tissue tolerator, while the second best tolerator, MDR 308, has good Na^+ exclusion. It is clear, though, that both of those accessions are also good osmotic tolerators. It appears that all of the lines with two tolerance mechanisms – either tissue tolerance with osmotic tolerance or Na^+ exclusion with osmotic tolerance – have greater whole-plant tolerance than other lines which appear to use only one tolerance mechanism.

The results presented in this paper also indicate that it may be difficult for plants to have both good Na^+ exclusion and good Na^+ tissue tolerance. The two mechanisms appear to be mutually exclusive. This may be an inevitable consequence of the methods used to calculate tissue tolerance, or it may reflect the relatively modest Na^+ concentrations used in the current work, where Na^+ concentrations in excluding lines are not high enough for tissue tolerance mechanisms to be evident. Alternatively, it may be because good excluders have evolved low tissue tolerance because their effective exclusion mechanisms reduce their requirement for tissue tolerance. Further experiments with higher Na^+ concentrations and with transgenic lines with increased Na^+ sequestration will provide further light on this issue.

It is clear from the analyses presented in this paper that several components contribute to salinity tolerance in *T. monococcum*; tolerance cannot be linked solely to Na^+ exclusion.

CONCLUSIONS

Non-destructive sampling methods have been developed using commercially supplied image capture and processing technologies to characterize the three main salinity tolerance mechanisms in *T. monococcum*: Na^+ exclusion, osmotic tolerance and tissue tolerance. These three mechanisms can then be added to describe overall plant salinity tolerance. Although these plants achieve only limited salinity tolerance by using either tissue tolerance or Na^+ exclusion alone, the combination of one of those mechanisms with osmotic tolerance generates a plant with significant salinity tolerance.

ACKNOWLEDGMENTS

Funding provided by the Australian Research Council (M.T. & S.R.), and the University of Adelaide International Scholarship scheme (K.R.) is gratefully acknowledged, as is generous support by the Australian Centre for Plant Functional Genomics. The authors would like to thank Dr Yuri Shavrukov (ACPFG) and Dr Hai-Chun Jing (Rothamsted Research, Rothamsted, UK) for advice on which *T. monococcum* accessions to use and for providing the seed, and Dr Trevor Hancock for statistical advice. The authors would also like to thank Dr Rana Munns (CSIRO, Canberra, Australia) for helpful comments on the manuscript.

REFERENCES

Anker C.C., Buntjer J.B. & Niks R.E. (2001) Morphological and molecular characterisation confirm that *Triticum monococcum* s.s. is resistant to wheat leaf rust. *Theoretical and Applied Genetics* **103,** 1093–1098.

Apse M.P., Aharon G.S., Snedden W.A. & Blumwald E. (1999) Salt tolerance conferred by overexpression of a vacuolar Na^+/H^+ antiport in *Arabidopsis*. *Science* **285,** 1256–1258.

Bhandal I.S., Malik C.P. & Bourne G.H., Jeon K.W. & Friedlander M. (1988) Potassium estimation, uptake, and its role in the physiology and metabolism of flowering plants. *International Review of Cytology* **110,** 205–254.

Blaha G., Stelzl U., Spahn C.M.T., Agrawal R.K., Frank J. & Nierhaus K.H. (2000) Preparation of functional ribosomal complexes and effect of buffer conditions on tRNA positions observed by cryoelectron microscopy. *Methods in Enzymology* **317,** 292–306.

Brini F., Hanin M., Mezghani I., Berkowitz G.A. & Masmoudi K. (2007) Overexpression of wheat Na^+/H^+ antiporter *TNHX1* and H^+-pyrophosphatase *TVP1* improve salt- and drought-stress tolerance in *Arabidopsis thaliana* plants. *Journal of Experimental Botany* **58,** 301–308.

Byrt C.S., Platten J.D., Spielmeyer W., James R.A., Lagudah E.S., Dennis E.S., Tester M. & Munns R. (2007) HKT1;5-like cation transporters linked to Na^+ exclusion loci in wheat, *Nax2* and *Kna1*. *Plant Physiology* **143,** 1918–1928.

Cakmak I., Cakmak O., Eker S., Ozdemir A., Watanabe N. & Braun H.J. (1999) Expression of high zinc efficiency of *Aegilops tauschii* and *Triticum monococcum* in synthetic hexaploid wheats. *Plant and Soil* **215,** 203–209.

Davenport R.J., Munoz-Mayor A., Jha D., Essah P.A., Rus A.N.A. & Tester M. (2007) The Na^+ transporter AtHKT1;1 controls retrieval of Na^+ from the xylem in *Arabidopsis*. *Plant, Cell & Environment* **30,** 497–507.

Dubcovsky J., Luo M.C., Zhong G.Y., Bransteitter R., Desai A., Kilian A., Kleinhofs A. & Dvorak J. (1996a) Genetic map of diploid wheat, *Triticum monococcum* L., and its comparison with maps of *Hordeum vulgare* L. *Genetics* **143,** 983–999.

Dubcovsky J., María G.S., Epstein E., Luo M.C. & Dvorák J. (1996b) Mapping of the K^+/Na^+ discrimination locus *Kna1* in wheat. *Theoretical and Applied Genetics* **92,** 448–454.

Flowers T.J., Hajibagherp M.A. & Yeo A.R. (1991) Ion accumulation in the cell walls of rice plants growing under saline conditions: evidence for the Oertli hypothesis. *Plant, Cell & Environment* **14,** 319–325.

Forster B. (2001) Mutation genetics of salt tolerance in barley: an assessment of Golden Promise and other semi-dwarf mutants. *Euphytica* **120,** 317–328.

Fricke W. & Peters W.S. (2002) The biophysics of leaf growth in salt-stressed barley. A study at the cell level. *Plant Physiology* **129,** 374–388.

Garthwaite A.J., von Bothmer R. & Colmer T.D. (2005) Salt tolerance in wild *Hordeum* species is associated with restricted entry of Na^+ and Cl^- into the shoots. *Journal of Experimental Botany* **56,** 2365–2378.

Gaxiola R.A., Li J., Undurraga S., Dang L.M., Allen G.J., Alper S.L. & Fink G.R. (2001) Drought- and salt-tolerant plants result from overexpression of the *AVP1* H^+-pump. *Proceedings of the National Academy of Sciences of the United States of America* **98,** 11444–11449.

Genc Y., McDonald G.K. & Tester M. (2007) Reassessment of tissue Na^+ concentration as a criterion for salinity tolerance in bread wheat. *Plant, Cell & Environment* **30,** 1486–1498.

Gorham J. (1990) Salt tolerance in the Triticeae: K/Na discrimination in synthetic hexaploid wheats. *Journal of Experimental Botany* **41,** 623–627.

Hasegawa P.M., Bressan R.A., Zhu J.-K. & Bohnert H.J. (2000) Plant cellular and molecular responses to high salinity. *Annual Review of Plant Physiology and Plant Molecular Biology* **51,** 463–499.

Hu Y., Burucs Z., von Tucher S. & Schmidhalter U. (2007) Short-term effects of drought and salinity on mineral nutrient distribution along growing leaves of maize seedlings. *Environmental and Experimental Botany* **60,** 268–275.

James R.A., Rivelli A.R., Munns R. & Caemmerer S.V. (2002) Factors affecting CO_2 assimilation, leaf injury and growth in salt-stressed durum wheat. *Functional Plant Biology* **29,** 1393–1403.

James R.A., Davenport R.J. & Munns R. (2006) Physiological characterization of two genes for Na^+ exclusion in durum wheat, *Nax1* and *Nax2*. *Plant Physiology* **142,** 1537–1547.

James R.A., von Caemmerer S., Condon A.G., Zwart A.B. & Munns R. (2008) Genetic variation in tolerance to the osmotic stress component of salinity stress in durum wheat. *Functional Plant Biology* **35,** 111–123.

Knox A., Li C., Vágújfalvi A., Galiba G., Stockinger E. & Dubcovsky J. (2008) Identification of candidate CBF genes for the frost tolerance locus Fr-A m 2 in *Triticum monococcum*. *Plant Molecular Biology* **67,** 257–270.

Møller I.S. & Tester M. (2007) Salinity tolerance of *Arabidopsis*: a good model for cereals? *Trends in Plant Science* **12,** 534–540.

Munns R. (2002) Comparative physiology of salt and water stress. *Plant, Cell & Environment* **25,** 239–250.

Munns R. & James R.A. (2003) Screening methods for salinity tolerance: a case study with tetraploid wheat. *Plant and Soil* **253,** 201–218.

Munns R. & Rawson H.M. (1999) Effect of salinity on salt accumulation and reproductive development in the apical meristem of wheat and barley. *Functional Plant Biology* **26,** 459–464.

Munns R. & Tester M. (2008) Mechanisms of salinity tolerance. *Annual Review of Plant Biology* **59,** 651–681.

Munns R., James R.A. & Lauchli A. (2006) Approaches to increasing the salt tolerance of wheat and other cereals. *Journal of Experimental Botany* **57,** 1025–1043.

Pardo J.M., Cubero B., Leidi E.O. & Quintero F.J. (2006) Alkali cation exchangers: roles in cellular homeostasis and stress tolerance. *Journal of Experimental Botany* **57,** 1181–1199.

Passioura J.B. & Munns R. (2000) Rapid environmental changes that affect leaf water status induce transient surges or pauses in leaf expansion rate. *Functional Plant Biology* **27,** 941–948.

Poustini K. & Siosemardeh A. (2004) Ion distribution in wheat cultivars in response to salinity stress. *Field Crops Research* **85,** 125–133.

Qiu Q.-S., Guo Y., Dietrich M.A., Schumaker K.S. & Zhu J.-K. (2002) Regulation of SOS1, a plasma membrane Na^+/H^+ exchanger in *Arabidopsis thaliana*, by SOS2 and SOS3. *Proceedings of the National Academy of Sciences of the United States of America* **99,** 8436–8441.

Ren Z.-H., Gao J.-P., Li L.-G., Cai X.-L., Huang W., Chao D.-Y., Zhu M.-Z., Wang Z.-Y., Luan S. & Lin H.-X. (2005) A rice quantitative trait locus for salt tolerance encodes a sodium transporter. *Nature Genetics* **37,** 1141–1146.

Rogers W.J., Miller T.E., Payne P.I., Seekings J.A., Sayers E.J., Holt L.M. & Law C.N. (1997) Introduction to bread wheat (*Triticum aestivum* L.) and assessment for bread-making quality of alleles from *T. boeoticum* Boiss. ssp. *thaoudar* at Glu-A1 encoding two high-molecular-weight subunits of glutenin. *Euphytica* **93,** 19–29.

Rus A., Baxter I., Muthukumar B., Gustin J., Lahner B., Yakubova E. & Salt D.E. (2006) Natural variants of AtHKT1 enhance Na^+ accumulation in two wild populations of *Arabidopsis*. *PLoS Genetics* **2,** 1964–1973.

Schachtman D.P. & Munns R. (1992) Sodium accumulation in leaves of *Triticum* species that differ in salt tolerance. *Functional Plant Biology* **19,** 331–340.

See D.R., Giroux M. & Gill B.S. (2004) Effect of multiple copies of puroindoline genes on grain softness. *Crop Science* **44,** 1248–1253.

Shi H., Quintero F.J., Pardo J.M. & Zhu J.-K. (2002) The putative plasma membrane Na^+/H^+ antiporter SOS1 controls long-distance Na^+ transport in plants. *The Plant Cell* **14,** 465–477.

Shi H., Lee B.-H., Wu S.-J. & Zhu J.-K. (2003) Overexpression of a plasma membrane Na^+/H^+ antiporter gene improves salt tolerance in *Arabidopsis thaliana*. *Nature Biotechnology* **21,** 81–85.

Sodkiewicz W. (2002) Diploid wheat – *Triticum monococcum* as a source of resistance genes to preharvest sprouting of triticale. *Cereal Research Communications* **30,** 323–328.

Sodkiewicz W., Strzembicka A. & Apolinarska B. (2008) Chromosomal location in triticale of leaf rust resistance genes introduced from *Triticum monococcum*. *Plant Breeding* **127,** 364–367.

Sunarpi H.T., Motoda J., Kubo M., *et al.* (2005) Enhanced salt tolerance mediated by AtHKT1 transporter-induced Na^+ unloading from xylem vessels to xylem parenchyma cells. *The Plant Journal* **44,** 928–938.

Tester M. & Davenport R. (2003) Na^+ tolerance and Na^+ transport in higher plants. *Annals of Botany* **91,** 503–527.

Wei W., Bilsborrow P.E., Hooley P., Fincham D.A., Lombi E. & Forster B.P. (2003) Salinity induced differences in growth, ion distribution and partitioning in barley between the cultivar Maythorpe and its derived mutant Golden Promise. *Plant and Soil* **250,** 183–191.

Yeo A.R., Lee S., Izard P., Boursier P.J. & Flowers T.J. (1991) Short- and long-term effects of salinity on leaf growth in rice (*Oryza sativa* L.). *Journal of Experimental Botany* **42,** 881–889.

Zhu G.Y., Kinet J.M. & Lutts S. (2001) Characterization of rice (*Oryza sativa* L.) F3 populations selected for salt resistance. I. Physiological behaviour during vegetative growth. *Euphytica* **121,** 251–263.

Received 10 September 2008; received in revised form 3 November 2008; accepted for publication 3 November 2008

SUPPORTING INFORMATION

Additional Supporting Information may be found in the online version of this article:

Figure S1. Non-destructive growth analysis techniques. (a) Plants were grown in a supported hydroponics system in 25 L tanks above an 80 L storage reservoir. (b) Plants were placed in a LemnaTec Scanalyzer for image acquisition. (c–h) Snapshots of original and false colour images of 31-day-old MDR 043 accession in 75 mM NaCl.

Table S1. Two-phase growth response of *Triticum monococcum* accessions. Mean relative plant growth rates are calculated between the day indicated, for both 0 and 75 mM NaCl conditions, and differences in growth rate ratios (G.R.) calculated (n = 7–10). Plants grown in winter[1]; plants grown in spring[2].

Table S2. Comparison of the two methods for generating an osmotic tolerance index. Mean relative growth rates were calculated for 0 and 75 mM grown plants, before and after salt application, as described in Fig. 3a, to generate two osmotic tolerance indices for comparison.

Table S3. The sources of accessions used in the study.

Please note: Wiley-Blackwell are not responsible for the content or functionality of any supporting materials supplied by the authors. Any queries (other than missing material) should be directed to the corresponding author for the article.